Copyright © 2012 Tech Science Press CMC, vol.27, no.3, pp.211-229, 2012

FEM Modeling of the Interface Strength and Its Effect on the Deformation Behaviour of Aluminum Cenosphere Syntactic Foam

Raghvendra Khedle[1], D.P.Mondal[2], S.N.Verma[1] and Sanjay Panthi[2]

Abstract: The interface in aluminum cenosphere syntactic foam (ACSF) is modeled using FEM to study its deformation behaviour as a function of interface characteristics such as interface stiffness and thickness. The interface is modeled as a thin layer of object. The effective modulus and stress of ACSF examined when it contain 50% cenosphere by volume. In this study, the shell wall thickness of cenosphere is fixed at 1μm. The width of the interface varies from 0.2% to 0.6% of cenosphere volume fraction. The interface strength and modulus varies in the range of 10 to 50% of the matrix alloy. The values of the normalized yield stress and the modulus decrease with increase in the interface width and decrease in the interface strength. The FEM predicted values are also validated with experimental value. The proposed study shows that unit representative shell techniques are reasonably ideal and fast method for predicting compressive deformation behaviour of ACSF.

Nomenclatures

ACSF	Aluminium cenosphere syntactic foam
σ	Flow stress (MPa)
σ_y	Yield strength(GPa)
ε	Effective strain
ε_y	Effective yield strain
n	Strain hardening exponent
σ_{ACSF}/σ_m	Normalized yield stress
E_{ACSF}/E_m	Normalized Young's modulus
σ_i/σ_m	Normalized strength of interface
T	Thickness of cenosphere (μm)

[1] Rajiv Gandhi Prodyogiki Vishwavidyalaya, Air Port Road, (Mechanical department), Madhya Pradesh, Bhopal, India, raghvendra056@yahoo.com, 9907729613, zipcode-462003

[2] Advanced Materials and Processes Research Institute (CSIR-AMPRI), Madhya Pradesh, Bhopal, India. mondaldp@yahoo.com, zipcode-462026

I.T	Interface thickness (μm)
FEM	Finite element modeling

1 Introduction

The metal matrix composites (MMCs), has wide range of application in aerospace and automobile due to there excellent combination of physical, tribological and mechanical properties [Vogelsang, Fisher and Arsenault (1986); Wang and Zhang (1991); Wang, Chen and Liyod (1993); Hirth (1991)]. In metal matrix composites (MMCs), the reinforcing phase is hard and the matrix is relatively soft. The incoherence between the respective constituents brings strong interaction effect that result at the interfacial region between the matrix and the reinforcing phase. This affects the deformation behavior of MMCs. In addition, the strong coherence between the matrix and the reinforcing phase play an important role in transferring the load from the matrix to the reinforcing phase and vice-versa. The interface influences the deformation behaviour of MMCs, depending on the bonding characteristic between the matrix, reinforcing phase and its thickness. This type of investigation has been studied by several investigators in metal matrix composites [Vogelsang, Fisher and Arsenault (1986); Wang and Zhang (1991); Wang, Chen and Liyod (1993); Hirth (1991); Atkin and Cristodoulou (1991); Lewandowski, Liu and Liu (1991), Kamat, Rollet and Hirth (1991); Vedani, Gariboldi, Silva and Digregorio (1994)]. The effect of size, shape, volume fraction and distribution of the constituent phases on its deformation behaviour has been examined [Vogelsang, Fisher and Arsenault (1986); Wang and Zhang (1991); Wang, Chen and Liyod (1993); Hirth (1991); Atkin and Christodoulou (1991); Ramakrishnana (1966), Lewandowski, Liu and Liu (1991), Kamat, Rollet and Hirth (1991);Verma,Kamat and Kutumbarao(2001)]. Several attempts have been made to understand the plastic flow behaviors of matrix in metal matrix composites [Hirth (1991); Atkin, and Christodoulou (1991); Ramakrishnana (1966), Lewandowski, Liu and Liu (1991)]. But no attempt has been made to understand for the deformation behaviors of ACSFs. The matrix of ACSF is similar to that of MMCs. But the reinforcement in ACSFs are hollow spherical in nature. Thus there would have significant differences in the deformation behavior between ACSFs and MMCs.

In case of composite, different approaches have been used to predict its deformation behaviour. All these studies are based on the assumption of:-[i]a strong bonding between the particle and the matrix, [ii] ideal load transfer from matrix to the reinforcement, [iii] different interfacial phases depicting the nature of the interface is not considered. In most of the practical cases, the interface bonding is not so strong so that the load transfer across the interface is ideal. [Heinrich, Vananti and Kostorz (2001); Preuss, Rauchs, Withers, Maire and Buffiere (2002);; Lee, Maeng, Hong and Won (2003); Kennedy and Wyatt(2001);Aghdam and Falahatgar (2004);Silvain, Proult, Lahaya and Douin (2003);Vicens, Chedru and Chermant (2002)].Eventually it has been inferred from the observations that the interface bonding and its thickness varies depending on the matrix reinforcement system, processing parameters and processing routes. According to [Kennedy and Wyatt (2001)] the interface bonding strength varies in Al-TiCp with the processing route. They evaluated that the least deterioration of interface led to strong composites in cast conditions. As compared to gravity cast composite [Lewandowski, Liu and Liu (1991)], the squeeze cast composite renders stronger interface. The modulus and the work hardening rate of the composites however, decrease with the increases in deformation. Therefore it is expected that the presence of stress or strain field at the interface varies with the processing route and it play an important role in the deformation behaviors of composite in an MMC. To measure the interface strength [Wang and Zhang (1991)] experimental methods like push out test and synchrotron strain measurement were used. As the matrix and reinforcement are not coherent in most of the cases, the interface strength is expected to less than that of the matrix alloy [Preuss, Rauchs, Withers, Maire and Buffiere (2002)]. In a nut shell the correlation between the interface strength with the deformation behavior of MMCs has not been systematically examined nither experimentally nor numerically. Mondal, Ramakrishnan and Das (2006) examined the effect of interface strength and stiffness on the deformation behavior of MMCs using Finite Element Method. But to the best of our knowledge no attempt has been made to examine the interface characteristics between the microbaloons and the matrix on the deformation behavior of ACSF.

Several attempts have been made to study the deformation behavior of particle reinforced metal matrix composites using finite element method [Lee, Maeng, Hong and Won (2003); Aghdam and Falahatgar (2004);Oliveira, Cunda, Creus and Ochsner (2008);Mondal, Ramakrishnan and Das (2006); Kim, Tunvir and Cheon (2005);Balasivanandha prabhu, Karunamoorthy and Kandansamai (2004)]. [Lee, Maeng, Hong and Won (2003)] simulate the interface by the application of coulomb friction model. According to this model, the critical shear strength of the interfacial layer and the orientation of the interface modulate the strength of interface. [Oliveira, Cunda, Creus and Ochsner (2008)] simulated the cellular metal under compression test by using Gurson damage model. [Aghdam and Falahatgar (2004)] simulated by using a representative volume element technique and introduced the concept of varied interface characteristic by varying its mechanical and physical properties. [Mondal, Ramakrishnan and Das (2006)] simulated the interface in a metal matrix composite to study deformation behavior as a function of interface characteristics such as interface stiffness and interface thickness volume fraction as well as reinforcing phase. [Kim, Tunvir and Cheon (2005)] simulated the unloading modulus of closed cell Al-alloy foam under monotonic compression, which was accomplished with a multiple cell FE model having the unit cell morphology on cubic-spherical section arrangement. [Kim, Young and Jae (2010)] reported that the Mechanical and thermal properties of poly (lactic acid) (PLA)/mica and poly (butylene terephthalate) (PBT)/mica composites were investigated when a coupling agent was added. By inserting void elements between the polymers and the mineral particles the Influence of the interfacial adhesion was studied through finite element analysis (FEA).

[Zhang and Xia (2005)] analyzed the interphase damage for fiber reinforced composite laminates. The prediction of interphase damage and their influences on the global stress-strain relation were made by FEM analysis on micromechanical behavior using unit cell model. [Hwu, Kuo and Chen (2009)] proposed a unified expression for a near tip solution of interface corner in term of stress intensity factors. This analysis included corner of interface and the cracks at the interface between two dissimilar materials. The unified solution for solving interface problem is finally implemented numerically through several different interface problems.

To the best of our knowledge no attempt has been made to characterize the interface through its strength/stiffness and thickness to study their effects on the deformation behavior of ACSFs. The present work focuses on the study of the deformation behavior of ACSF as a function of the interface characteristics, such as interface thickness, strength and modulus using FEM of representative unit cell. In this study, the interface with varying strength/stiffness and thickness at fixed volume fraction of cenosphere has been considered. The smallest representative volume element was considered for the geometric modeling in FEM.

2 Finite element modelling

In the present study, the interface thicknesses as well as its mechanical properties are varied and the effective properties (yield stress and Young's modulus) are analyzed parametrically for same volume fractions of the reinforcement. The modelling and the analysis were executed using finite element software. The model assumes spherical particles of cenosphere distributed in Al-matrix uniformly and the interface in between aluminum and cenosphere. A mesh is considered as axial symmetry with a quarter of the representative unit cell as shown in Fig.1. To capture the steep gradients in stress and strain, (this is due to the sudden change in material properties across the interface), the mesh in the interface and the shells are finer in the radial direction, inside as well as either side of the interface cell wall. Cenosphere shell thickness is kept constant at 1μm and the cenosphere volume fraction of the cenosphere particle. This cenosphere volume fraction is fixed at 50%. The interface thickness varies in the range of 0.2% to 0.6% of the cenosphere volume fraction. The interface strength and modulus varies in the range of 10 to 50% of the matrix. Material properties used for FEM analysis are shown in Table 1.

Table 1: Material property used for FEM analysis.

S.No.	Property	Material-1	Material-2(Interface strength)					Material-3
		Aluminium matrix	10%	20%	30%	40%	50%	Cenosphere shell
01	Young's modulus GPa	70	7	14	21	28	35	112
02	Poisson's ratio	0.3	0.3	0.3	0.3	0.3	0.3	0.23
03	Strain Hardening	0.29	0.29	0.29	0.29	0.29	0.29	0.0
04	Yield Strength, MPa	260	26	52	78	104	130	560

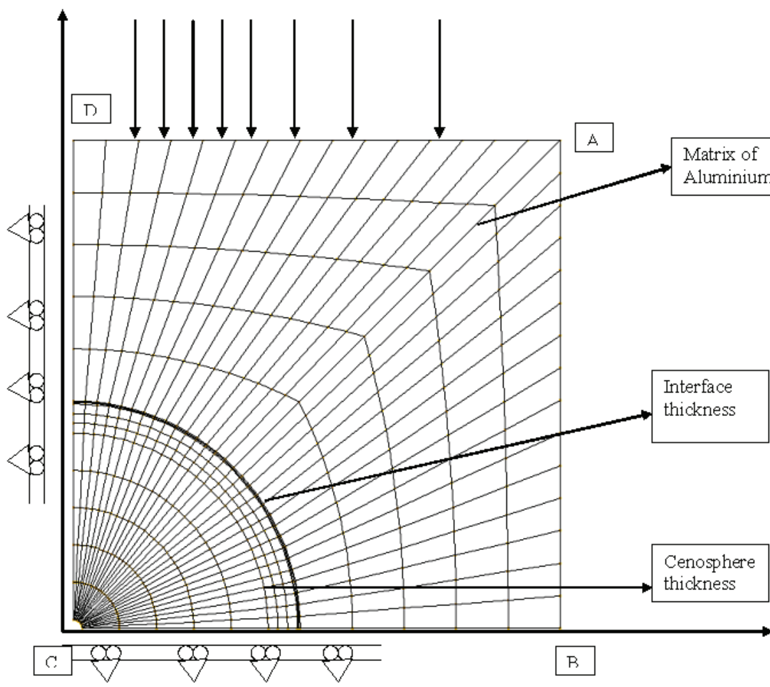

Figure 1: Unit cell model of ACSF with interface.

The boundary condition is specified taking into account the symmetry of the system. In Fig.1, the nodal displacement on CD is considered to be zero in the xdirection due to axial symmetry and CB is constrained in the y-direction representing plane of symmetry. Compressive displacements are applied to the top of horizontal surface AD. When displacement is applied in vertical direction to the top surface the vertical faces must continue to be vertical while the distance between them changes. The strain is applied incrementally to simulate the overall deformation of ACSF. The maximum displacement applied to the top surface is 10% of the total length at total number of steps of 100. These boundary conditions are applied to analyze parameters like strain, yield stress and Young's modulus in relation with interface characteristics. Von Mises yield criteria in conjunction with the following standard power law flow curve was used for the plastic deformation of the matrix:

$$\sigma/\sigma_y = (\varepsilon/\varepsilon_y)^n \tag{1}$$

Where σ, $\sigma_{y,}$ ε, ε_y and n are the flow stress, yield strength, effective strain, yield strain and strain hardening exponent of the material.

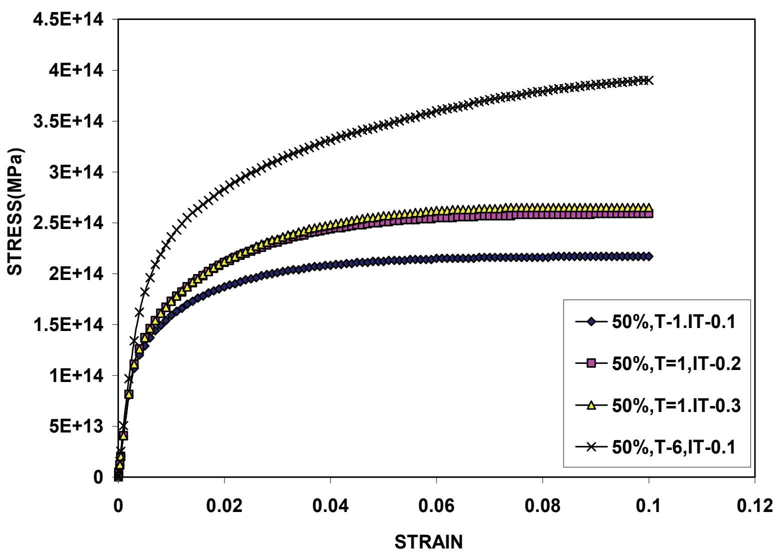

Figure 2: Flow curve at different interface thickness.

3 Result and discussion

3.1 Flow behavior

The flow curve as shown in Fig.2 depicts the relation between the true stress and true strain of ACSF at fixed cenosphere volume fraction of 50% and interface strength of 10% of the matrix alloy. At fixed volume fraction of cenosphere (50%) and varying thickness and strength of interface under unconstrained condition, the curves are derived from FEM. It is noted from these curves that none of the flow curves have sharp yield point. The material gradually changes from elastic to plastic region, without showing any sudden increases in stress irrespective of boundary condition. The important fact that the ACSF with lower interface thickness behaves like a conventional foam material (i.e. there is no significant increases of stress with strain). It is also noted that Young's modulus as well as flow stress decrease with increase in interface thickness. It is further noted that the strength of ACSF decreases with decrease in interface strength and its effect is more prominent when the interface strength is very low.

3.2 Effect of interface thickness and interface strength

It is noted from Fig.3 (a), that the normalized yield stress varies with normalized strength of interface for different interface thickness (0.2 to 0.6%).The normalized yield stress of ACSF increases with increases in the normalized strength of interface. It is interestingly noted that the effect of normalized interface strength of the ACSF is different under different interface thickness. In case of wider interface thickness (> 0.4%), the normalized yield stress increases very rapidly when normalized interface strength increases from 0.1 to 0.25, and after that it increases linearly with the normalized yield strength of the interface. But at thinner interface (<0.4%), the normalized yield stress of ACSF increases linearly with normalized strength of interface. In case of wider interface (> 0.4%) it is further noted that the increase in normalized yield stress of ACSF with normalized yield strength of interface slowed down when the interface strength is greater or equal 0.25. Beyond 25% normalized strength of interface, the normalized strength of ACSF follows a linear relationship with interface strength. This demonstrates that at least 25% of yield strength at the interface is need for obtaining sufficient strength of ACSF, especially where interface thickness is greater than 0.4%.

Fig.3 (b) represents the variation of normalized modulus of ASCF with normalized interface modulus. This figure shows that the normalized Young's modulus of ACSF increases with increase in normalized modulus of interface. It is further noted, that, for interface thickness <0.4%, the normalized strength ACSF increases linearly with normalized modulus of interface. But, for the interface thickness

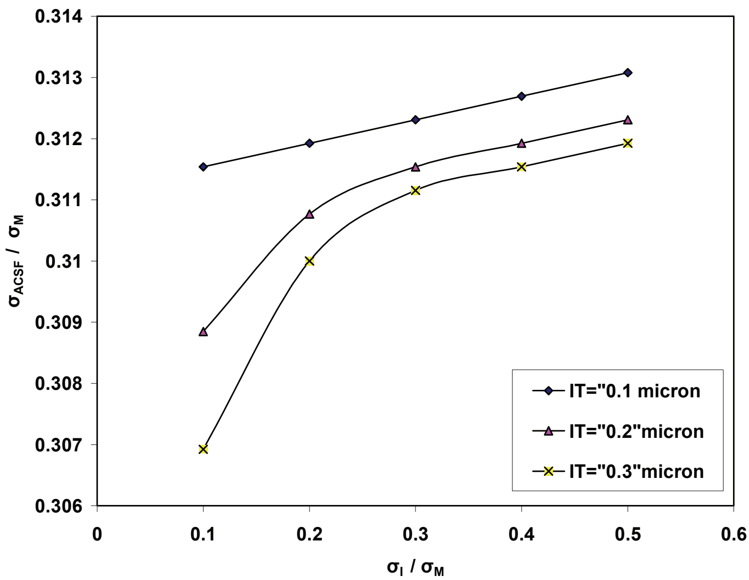

(a)

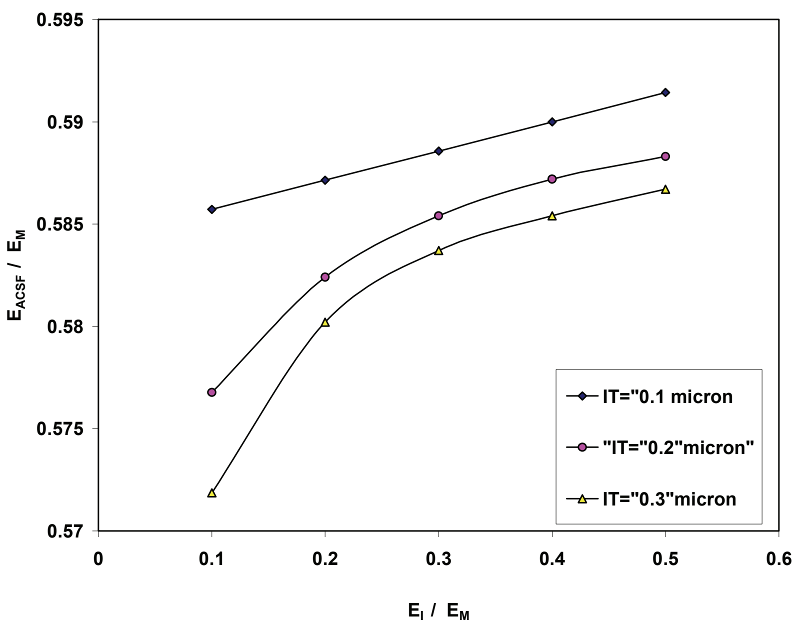

(b)

Figure 3: (a) Variation of normalized yield stress with normalized interface strength at different interface thickness. (b) Variation of normalized Young's modulus with normalized modulus of interface at different interface thickness.

greater than 0.4%, the modulus of ACSF increases rapidly when normalized interface modulus increases from 10% to 25%. Further increase in interface modulus leads to linear increment modulus of ACSF with that of interface, but at slower rate. This again confirm that an interface strength of 25% is reasonably good for getting significantly high strength and stiffness in ACSF. But it is to be noted that the overall variation in strength and stiffness is only by 2.5%. This is very nominal.

The Fig 4(a) and 4(b), show that the normalized yield stress and normalized Young's modulus, respectively, of ACSF varies with normalized interface thickness (interface thickness\radius of unit cell) at different interface strength (10 to 50%). It is noted from Fig 4(b), that the normalized Young's modulus decreases with increases in normalized interface thickness. Beyond 0.4%, interface thickness the curve appears to be gradually decreases its slope and indicating reaching towards a stable value. Similar kind of variation of normalized yield strength of ACSF with that of normalized interface thickness is examined as shown in Fig. 4(a). The overall variation in modulus is very marginal due to variation in Interface thickness (<2.5%). This also demonstrates that in ACSF, the strength and stiffness is not significantly influenced by the interface strength and interface characteristics.

However, within the present state of variation, it could be noted from the above discussion that the effectiveness of the interface on the normalized yield stress or normalized modulus of ACSF is a function of interface thickness and interface strength a modulus. This is in line with the observation made in case Al-matrix composites as reported elsewhere [Mondal, Ramakrishna and Das (2006)]. The interface effectiveness could be expressed using the following dimension parameters.

$$\eta_m = \ln \frac{E_i/E_m}{t_i/t_p} \tag{2}$$

$$\eta_s = \ln \frac{\sigma_i - \sigma_m}{t_i/t_p} \tag{3}$$

Where η_s and η_m are interface effectiveness towards strength and modulus of ACSF, respectively. E_i and E_m are the modulus of interface and modulus of the matrix respectively. σ_i is the interface strength. σ_m represents the strength of matrix respectively. t_i represents interface thickness and t_p in the shell thickness respectively.

The normalized modulus of ASF is plotted as a function of η_m as shown in Fig.5 (a). It is noted from this figure that normalized modulus of ACSF is a strong function of η_m. It is further noted that normalized modulus of ACSF reached to a stable value at $\eta_m \sim 1.0$. Similarly, Fig.5 (b) represents variation of normalized yield stress of ACSF as a function of η_s. It is evident from this figure that yield stress of ACSF reaches to a stable value at $\eta_s \sim 1$. These two figures demonstrate that both

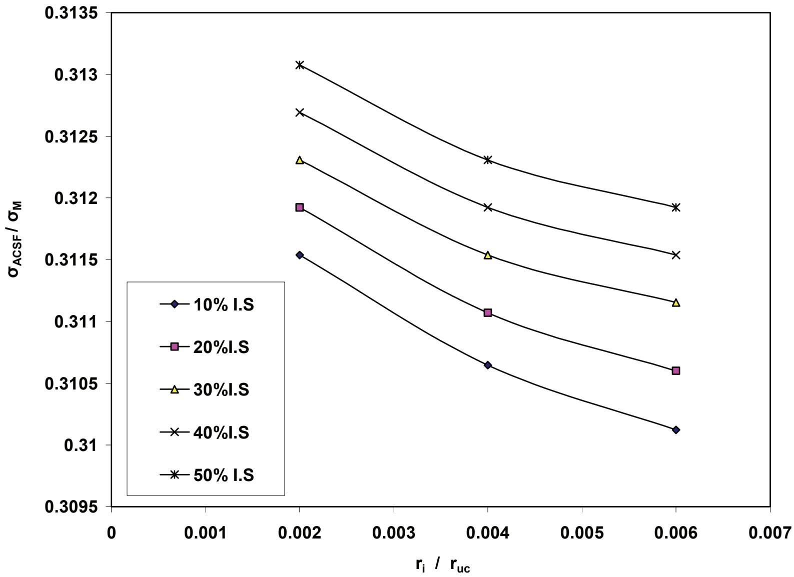

(a)

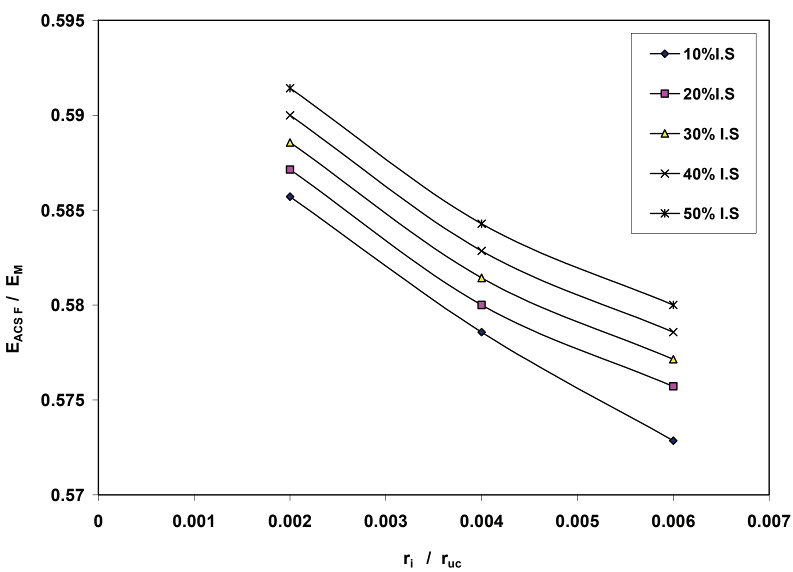

(b)

Figure 4: (a) Variation of normalized interface thickness with normalized yield stress at different interface strength. (b) Variation of normalized interface thickness with normalized Young's modulus at different interface strength.

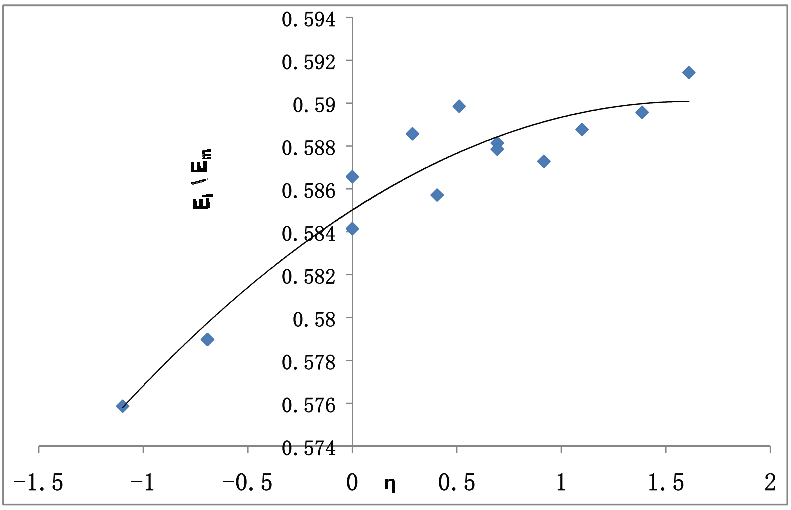

(a)

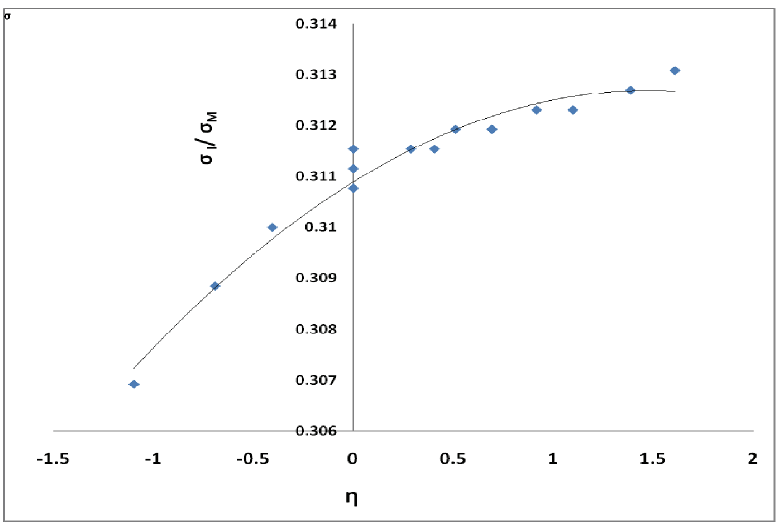

(b)

Figure 5: (a) The variation of the normalized effective modulus of the composite as a fraction of η Where η = 1n {E_i/ E_m) / (t_i/t_p}. (b) The variation of the normalized effective stress of the composite as a fraction of η Where η = 1n {(σ_i/σ_m) / (ti/t_p}.

modulus and yield stress of ACSF follow similar trend of variation with η_m and η_s respectively. It is understood from this analysis that at $\eta_s \approx \eta_m \approx 1.0$, the yield stress and the modulus of ACSF reaches to a stable value. Hence one must aims at attaining $\eta_s \approx \eta_m \approx 1.0$ for obtaining effective strengthening of ACSF. However, if one consider the overall variation in strength and modulus, it is understood that the variation is very marginal (less than 3.0%) even with significant variation of η. This is attributed to the fact that ACSF is a foam material. The interface thickness here is valued in the range of 0.2 to 0.6% which would lead to variation in porosities in ACSF by less than 2%. In case of foam, load is not effectively transferred through cenosphere as it contains more than 90% porosity. As a result, the interface only causes very minor variation in porosity in ACSF without any significant influence in the stress distribution as depicted in Fig.5 (b).

3.3 Stress-distribution

The effectives stress distribution in the representative unit cell for varying interface thickness and strength after deformation of 10% are shown in Fig. 6. It may be noted that the trend of stress distribution is almost same irrespective of interface thickness and interface strength. It is interesting to note that interface region is subjected to less tensile stress when the interface strength is 10% (Fig. 6(a)). The surface of cenosphere is subjected to more tensile stress with increases in interface strength (Fig. 6(b)). The stress distribution remains unchanged with the increases in interface thickness as shown in Fig .6(c) and Fig.6 (d). However, the absolute value of tensile stress decreases marginaly with increase in interface thickness and interface strength which is revealed from these figures. The maximum compressive stress (encountered at bulged region) decreases with increase in interface thickness and interface strength and stiffness. However, this variation is marginal. As a result, overall influence of interface thickness and strength (within the selected domain) on the deformation behavior of syntactic foam is insignificant. It is interesting to note that the centre line and the side of the cenosphere surface in the unit cell is subjected to compressive stress, while the region between these two regions are subjected to compressive stress. This will cause shear fracture of cenosphere cells while subjected to deformation. Thus, during deformation, the cenosphere shells will get shear followed by fragmentation and crushing and compaction.

3.4 Experimental validation

In order to change the interface thickness and stiffness, aluminum syntactic foam was made by permanent mould (cast iron) gravity cast and squeeze cast (at an applied pressure of 75MPa) because of application of pressure during solidification of ACSF in squeeze cast, it is expected that ACSF made through this process

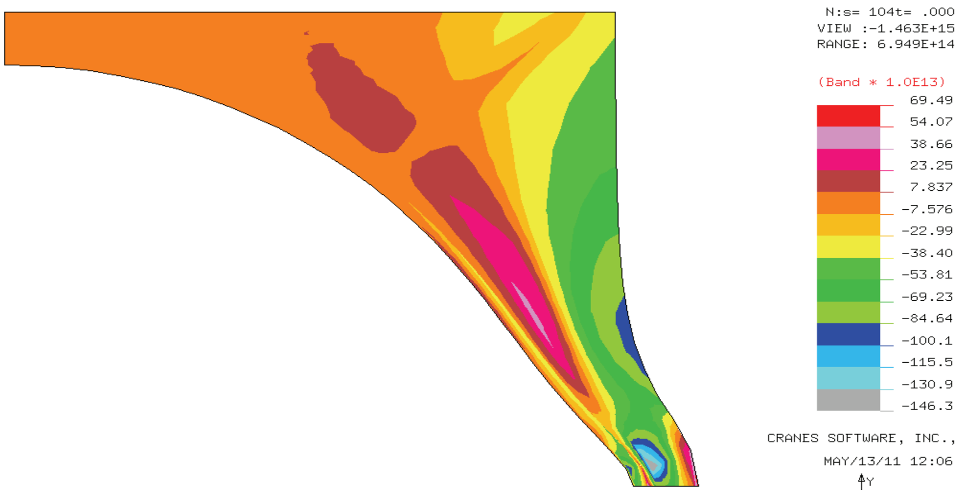
N:s= 104t= .000
VIEW :-1.463E+15
RANGE: 6.949E+14
(Band * 1.0E13)
69.49
54.07
38.66
23.25
7.837
-7.576
-22.99
-38.40
-53.81
-69.23
-84.64
-100.1
-115.5
-130.9
-146.3
CRANES SOFTWARE, INC.,
MAY/13/11 12:06
Y

(a)

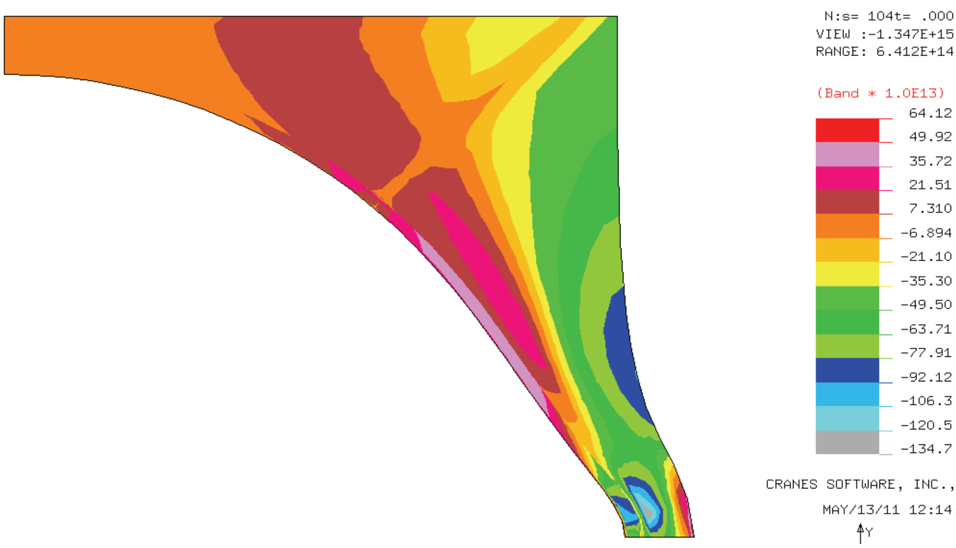
N:s= 104t= .000
VIEW :-1.347E+15
RANGE: 6.412E+14
(Band * 1.0E13)
64.12
49.92
35.72
21.51
7.310
-6.894
-21.10
-35.30
-49.50
-63.71
-77.91
-92.12
-106.3
-120.5
-134.7
CRANES SOFTWARE, INC.,
MAY/13/11 12:14:
Y

(b)

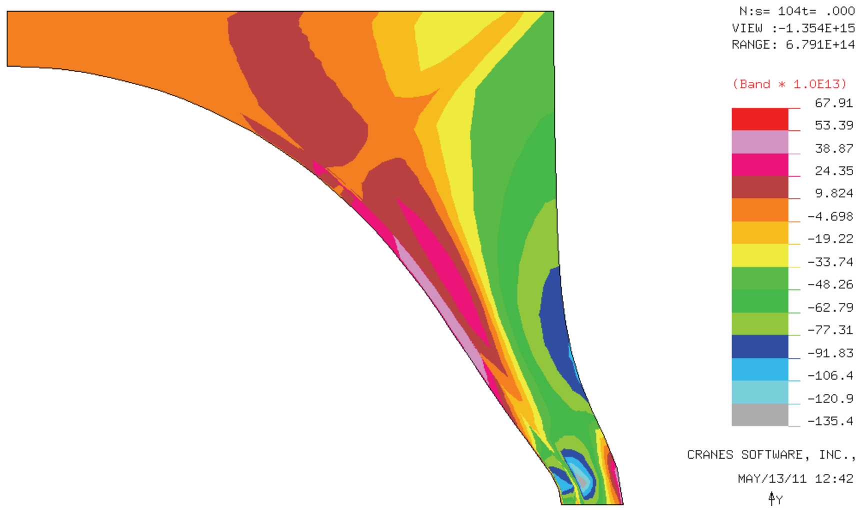

(c)

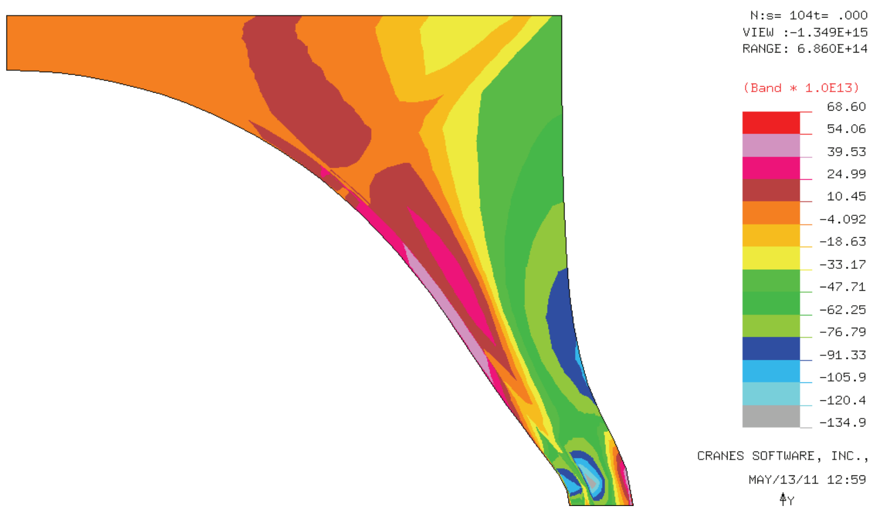

(d)

Figure 6: (a) Effective distribution of stress: in 50% volume fraction of cenosphere with 10% of strength of matrix and 0.2% normalized interface thickness. (b) Effective distribution of stress in 50% volume fraction of cenosphere with 50% of strength of matrix and 0.2 % normalized interface thickness. (c) Effective distribution of stress in 50% volume fraction of cenosphere with 50% of strength of matrix and 0.4 % normalized interface thickness. (d) Effective distribution of stress in 50% volume fraction of cenosphere with 50% of strength of matrix and 0.6% normalized interface thickness.

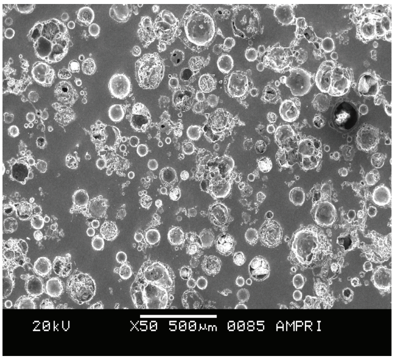

7(a)

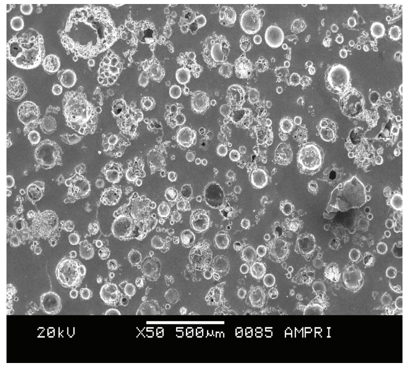

7(b)

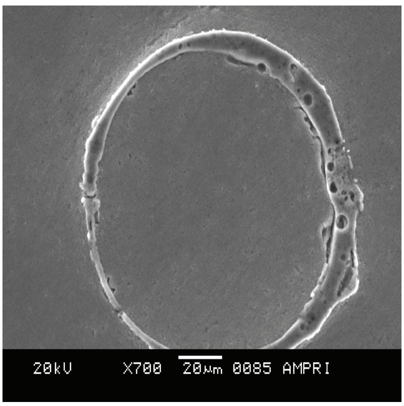

7(c)

7(d)

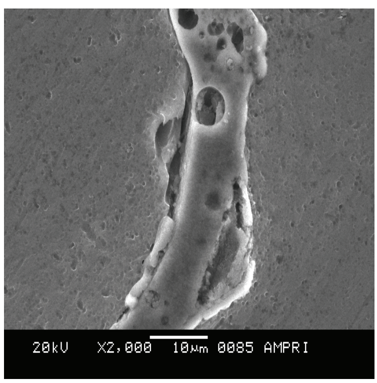

7(e)

Figure 7: Microstructure of ACSF: (a) Cenosphere distribution in squeeze cast, (b) Distribution of cenosphere in gravity cast, (c) Interface bonding between matrix and cenosphere in squeeze cast, (d) Interface bonding between matrix and cenosphere in gravity cast, (e) Bonding between cenosphere and matrix in gravity cast at higher magnification.

would provide stronger bonding with the matrix. The microstructure of ACSF made through squeeze cast and gravity cast are shown in Fig.7 (a) and Fig.7 (b) respectively. In both the cases, the cenospheres are uniformly distributed and the volume fraction of cenosphere is measured to be 50%. The higher magnification micrograph of ACSF made though squeeze casts and gravity cast are shown in Fig.7 (c) and Fig.7 (d) respectively. It is evident from Fig.7 (d) that the interface is very sharp and more intimate in case of squeeze cast. But, the interface in the case of gravity cast one is associated with weak bonding (mark arrow) in Fig.7(c). The micrograph of gravity cast ACSF at very high magnification is depicted in Fig.7 (e). It clearly demonstrates gap and micro porosity at the interface. It is noted that the squeeze cast one does not lead to any significant improvement in the yield strength even through the bonding strength in case of later one is stronger than the first one. The gravity cast ACSF exhibits interface gap in few locations. The micro-hardness measurement at the interface indirectly shows that the squeeze cast one have strong interface (140kg/mm^2) as compared to the gravity cast one(82 kg/mm^2). The plateau stress and densification strain of 50% cenosphere reinforced ACSF under gravity cast has been compared with that of squeeze cast one, at interface thickness of 1% and 4% and interface strength of 10% and 50% (Table 2). It is noted that the plateau stress and densification strain are improved very marginally even though the interface strength/stiffness is improved significantly during squeeze casting. This is exactly observed in the predicted valves through FEM. This is attributed to the fact that the analysis is made for a foam material, and the weak interface between cenosphere and matrix, here, acts as empty space. Variation of interface thickness between 0.2 to 0.4% does not significantly change the porosity of ACSF and being a porous materials it does not help in effective load transferring. This is also understood from the almost similar type of stress distribution irrespective of interface strength and modulus.

Table 2: Comparison of FEM results with Experimental value at 50% Cenosphere volume fraction.

S.No	Cenosphere interface thickness %	Interface strength%	Normalized Yield stress		Normalized Young's modulus	
			FEM	Experiment	FEM	Experiment
01	2	10	0.311538	0.298(gc)	0.585714	0.569(gc)
02	2	20	0.311923		0.587143	
03	2	30	0.312308		0.588571	
04	4	30	0.311154		0.58371	
05	4	50	0.311923	0.304(sc)	0.5867	0.575(sc)

4 Conclusion

The following conclusions could be made from this study.

1. The unit representative cell methodology could be successfully applied for predicting deformation response of Al-cenosphere syntactic foam.

2. The stress and strain distribution remains almost unchanged with interface strength/stiffness and interface thickness.

3. Interface strength /stiffness >25% of the matrix does not lead to any further improvement in plateau stress and modulus of the ACSF. In fact, the effect of interface strength and stiffness on the strength and stiffness of ACSF is almost insignificant (variation is less than 3%).

4. A simple parameter 'η', the interface effectiveness could be used for designing ACSF with required plateau stress and stiffness. Attempts to be made for attaining $\eta \sim 1.0$.

5. Squeeze cast and gravity cast ACSF exhibits almost similar strength and stiffness. This is because of the fact that bonding between cenosphere and matrix is irrelevant in the case of foams particularly for its deformation behavior.

References

Atkin, M. R.; Christodoulou, L. (1991): The role of equiaxial particles on the yield stress of composites. *Scripta Metallurgica et Materialia*, vol. 25, no. 1, pp. 9-14.

Aghdam, M. M.; Falahatgar, S. R. (2004): Mechanical behaviour of cast particles Sic/Al (A356) metal matrix composites. *Composites structure*. Vol.66, no.1-4, pp.415-420.

Balasivanandha prabhu, S.; Karunamoorthy, L.; Kandansamai, G.S. (2004): A finite element analysis study of micromechanical interfacial characteristics of metal matrix composites. *Material Processing Technology*, vol. 153-154, pp. 992-994.

Hirth, J.P. (1991): Introduction to the view point set on the mechanical properties of Al-matrix particulate composites. *Scripta Metallurgica et Materialia*, vol. 25, no. 1, pp. 1-2.

Hwu, C, ; Kuo, T.L.; Chen, Y.C.; (2009): Interfaces between two dissimilar elastic materials. *CMC: Computers, Materials, & Continua.* vol.11, no. 3, pp.165-183

Heinrich, H.; Vananti, A.; Kostorz, G. (2001): Strain fields at interface of Al-based Metal Matrix composites. *Material Science and Engineering A,* Vol. 321, no. 1, pp. 434-438.

Kamat, S.V.; Rollet,A.D.; Hirth,J.P. (1991): Plastic deformation in Al-alloy matrix-alumina particulates composites. . *Scripta Metallurgica et Materialia*, vol. 25, no. 1, pp. 27-32.

Kennedy, A. R.; Wyatt, S. M. (2001): Characterising particle matrix interfacial bonding in particulate Al-TiC MMCs produced by different methods. *Composites Part A:Applied Science and Manufacturing*, vol. 32, no. 3-4 pp 555-559.

Kim, A.; Tunvir, K.; Cheon,S.S. (2005): Study on the unloading modulus of Al-alloy foam by FE Modeling .ICME05-AM-37., pp.28-30.

Kim, M. W.; Young, S. S.; Jae, R. Y. (2010): Effects of interfacial adhesion and crystallization on the thermoresistance of poly (lactic acid)/mica composites. *Composites Part A: Applied Science and Manufacturing,* Vol. 41, no. 12, pp. 1817-1822

Lewandowski, J.J.; Liu, D. S.; Liu, C. (1991): Observations on the effect of particulate size and superposed pressure on deformation of metal matrix. *Scripta Metallurgica et Materialia*, vol. 25, no. 1, pp. 21-26.

Lee, J.H.; Maeng, D. Y.; Hong, S. I.; Won, C. W. (2003): Prediction of cracking modes and hardening behaviour of MMC via FEM. *Material Science and Engineering A,* Vol. 339, no. 1-2, pp. 175-182.

Mondal, D. P.; Ramakrishnan, N.; Das, S. (2006): FEM modeling of the interface and its effect on the elastio-plastic behavior of metal matrix composites. *Material Science and Engineering A,* Vol. 433, no. 1-2, pp. 286-290.

Oliveira, F.B.; Cunda, B.B.L.A.; Creus, J. G.; Ochsner, A. (2008): Finite element simulation of compression tests on cellular metals. *Sepex.*

Preuss, M.; Rauchs, G.; Withers, P.J.; Maire, E.; Buffiere, J.Y. (2002): Interfacial shear strength of Ti/SiC fibre composite measured by synchrotron strain measurement. *Composites Part A: Applied Science and Manufacturing*, vol. 33, no. 10, pp 1381-1385.

Silvain, J. F.; Proult, A.; Lahaya , M.; Douin, J. (2003) : Microstructures and chemical analysis of C/cu/Al interfacial zones. *Composites Part A: Applied Science and Manufacturing* , vol. 34, no. 12, pp. 1143- 1149.

Vogelsang, M.; Fisher, R. M.; Arsenault, R. J. (1986): Anin situ HVEM study of dislocation generation at Al/SiC interfaces in metal matrix composites. *Metallurgical Transaction A*. vol. 17, no. 3, pp. 379- 388.

Vicens, J.; Chedru, M.; Chermant, J.L. (2002): New Al-Ain composites fabricated by squeeze casting interfacial phenomena, *Composites Part A: Applied Science and Manufacturing*, vol. 33, no. 10, pp. 1421- 1423.

Vedani, M.; Gariboldi, E.; Silva, G.; Digregorio, E. (1994): Influence of interface properties on mechanical behaviour of particle reinforced metal matrix composite. *Material Science and Technology*. vol.10, no. 2, pp.132-140.

Wang , Z.; Zhang, R.J. (1991): Mechanical behaviour of cast particulate SiC/Al (A356) metal matrix composites. *Metallurgical Transaction A*.,vol. 22, no. 7, pp.,1585-1593.

Wang, Z.; Chen, T.; Llyod, D.J. (1993): Stress distribution in particulate reinforced metal matrix composites subjected to external load. *Metallurgical Transaction A*., vol. 24, no. 3, pp.197-207

Zhang,Y; Xia,Z; (2005): Micromechanical analysis of interphase damage for fiber reinforced composite laminates. *CMC: Computers, Materials, & Continua.* vol.2, no. 3, pp.213-226